

Laves phase precipitation and sigma phase transformation in a duplex stainless steel microalloyed with niobium.

Wandercleiton da Silva Cardoso¹
Raphael Colombo Baptista²

¹PhD program in Civil, Chemical and Environmental Engineering, Curriculum in Chemical, Materials and Process Engineering, Department of Chemical, Civil and Environmental Engineering (DICCA), Università degli Studi di Genova, Via All'Opera Pia, 15, CAP 16145, Genoa, Italy

²Postgraduate Program in Metallurgical and Materials Engineering (PROPEMM), Department of Metallurgy and Materials, Instituto Federal do Espírito Santo (IFES), Av. Vitória, 1729 - Jucutuquara, Vitória/ES, Brazil, CEP 29040-780
e-mail: wandercleiton.cardoso@dicca.unige.it, colombo.rafael@hotmail.com

ABSTRACT

Duplex stainless steels are used to replace austenitic steels in industrial applications, especially in the chemical industry where corrosion resistance in chloride-containing media is an important requirement. According to literature, niobium has a great influence on the transformation of the phases of these steels (ferrite, austenite and sigma). Given the interest in evaluating this property in terms of wear resistance and corrosion of the material, the aim of this study was to evaluate the effect of niobium on the formation in austenitic-ferritic stainless steel SEW 410 Nr 1.4517 after heat treatment at 850°C for 15, 30 and 60 minutes. The niobium contents studied were 0.2; 0.5 and 1.5 wt%. Measurements of microhardness, electrochemical tests in saline solution containing 3.5% sodium chloride and wear resistance were carried out. The results show that an increase in niobium content and sigma phase leads to an increase in hardness and wear resistance, associated with a decrease in corrosion potential. Therefore, the use of niobium in austeno-ferritic stainless steel is recommended when wear resistance is an important factor to be considered.

Keywords: Duplex stainless steel, Niobium, Sigma Phase, Laves Phase, Chemical Industry.

1. INTRODUCTION

Stainless steels are materials used in a wide variety of applications, including the chemical and petrochemical industries, power generation, pumps, implants, and surgical instruments, as well as a variety of other consumer and commercial products [1-6].

Chromium (Cr) is an alpha element responsible for forming the passive film in stainless steels that protects them from corrosion. Molybdenum (Mb) is the element that acts as a stabilizer in the ferritic phase and has a great influence on the passivity and corrosion resistance of stainless steels, especially in the presence of chloride ions, to which the passivity of chromium is not very stable. The addition of nickel (Ni) causes a change in the structure of the material and increases the range of the austenite phase. Nitrogen (N) is used in stainless steels to stabilize the austenitic phase and increase corrosion resistance [7-9].

Niobium (Nb) favors the formation of ferrite as it combines with carbon (C) and nitrogen, the stabilizing elements of austenite, dissolving them from the matrix and forming precipitates and intermetallic compounds, the marked weakening effect being displaced by the positive effect of refining the ferritic grain [10].

The main phases in duplex stainless steels are austenite (γ) and ferrite (α). Heating these steels to temperatures of 600° to 850°C leads to a reduction in ferrite content (α) and to the formation of the sigma phase (σ), a very common intermetallic compound that has a greater effect on the mechanical properties of the material and significantly reduces ductility and notched impact strength. It forms preferentially at the interface between ferrite and austenite, which is stable up to a maximum temperature of 1050°C [11-14].

Another intermetallic precipitate that forms in stainless steels containing niobium is the *Laves phase*, in which iron can be replaced by chromium, especially in super-stoichiometric compositions, appearing in the form of lamellae in the matrix and weakening the metal alloy [15-19].

In corrosion processes, metals react with non-metallic elements such as oxygen (O₂), sulfur (S), hy-

drogen sulfide (H₂S), and carbon dioxide (CO₂) present in the medium to form compounds similar to those in nature from which they are derived. The presence of chromium, molybdenum and nitrogen favors the pitting corrosion resistance of stainless steels and the performance of duplex stainless steels, which can be evaluated using the empirical formula PREN (Pite Resistance Equivalent Number) [20, 21]. If this value is above 40, the duplex stainless steels are called "super-duplex" according to Equation 1.

$$\text{PREN} = \% \text{Cr} + 3,3 (\% \text{Mo} + 0,5\% \text{W}) + 2 (\% \text{Cu}) + 16 (\% \text{N}) \quad (1)$$

Despite the good correlation between the PREN expression and the results of various corrosion tests, the equation must be used qualitatively to establish an approximate ranking between different steels. In the case of duplex stainless steels, it is important to consider the corrosion resistance of the two phases (ferrite and austenite), since there are differences in the content of alloying elements [22].

Corrosion in duplex stainless steels results from the breakdown of the passive film in the presence of chloride ions, which form soluble chloride-metal complexes when the base metal is exposed to the corrosive medium. Wear is defined as the loss of material due to relative movement between two contact surfaces. There are different types of wear such as abrasion, corrosion, adhesion, erosion and fatigue, which are affected by the environment, temperature, loading conditions and contact area. The wear coefficient (K) can be calculated using the Archard equation, according to Equation 2.

$$K = (\pi b^4)/(32\phi LF_N) \quad (2)$$

Where "b" is the diameter of the wear cap as determined by an optical microscope attached to the equipment and the diameter of the test ball, "L" is the distance traveled by the ball, and "F_N" is the force exerted by the ball and "φ" is the diameter of the wear sphere [23].

Generally, duplex stainless steels are used as substitutes for austenitic stainless steels, especially in the chemical industry when higher corrosion resistance and mechanical strength in a chloride-containing aqueous medium are required.

In this work, the effect of niobium on the microstructure of super-duplex stainless steel SEW 410 Nr. 1.4517 was evaluated after thermal treatments considering different element contents and heating times in previously prepared samples. Microhardness measurements and corrosion and wear tests were carried out to quantify the effect of the element on the steel.

2. MATERIALS AND METHODS

The material used in this work was SEW 410 W. Nr. 1.4517 duplex stainless steel with different additions of niobium. Twelve specimens were used, 4 samples with 0.2Nb, 4 samples with 0.5%Nb and 4 samples with 1.5%Nb.

2.1 Chemical composition

The chemical compositions of the samples were determined using an Oxford Instruments optical emission spectrometer, model Foundry-Master Pro. The super-duplex stainless steel used in the study, SEW 410 W. Nr. 1.4517, contained additions of niobium in the contents of 0.2%, 0.5% and 1.5%Nb.

The content of 0.2 wt% niobium corresponds to the value required to stabilize the carbon according to the stoichiometry of niobium carbides (NbC e Nb₄C₃).

The content of 0.5%Nb was chosen because this is normally the maximum allowable value for chemical elements not listed in the standards, and finally 1.5% Nb to highlight and clarify the effects of this element on the microstructure of duplex stainless steel.

2.2 Heat treatments

The 12 samples were first heated to 1050°C and held in an oven for 60 minutes to dissolve precipitates and intermetallic phases in the microstructure of the material. In the aging heat treatment, 9 samples were heated again to a temperature of 850°C and held for 15, 30 and 60 minutes [3, 11]. In this way, 12 different samples were prepared. After the heat treatment was completed, the oven was turned off and the sample was cooled slowly inside the equipment itself.

2.3 Microstructural analysis

Behara reagent (25ml HCl, 3g ammonium bifluoride, 125ml H₂O, and 0.4g potassium metabisulfite) was used to reveal the microstructure of the dissolved and aged samples.

The micro-components were analyzed in an XL30 FEG field emission scanning electron microscope. The sigma (σ), ferrite (α), and austenite (γ) phases were quantified using images from 60 different fields with a Fischer model FMP30 Ferritoscope.

2.4 Hardness measurements

Hardness measurements were performed using an OTTO WOLPERT WERK durometer with a diamond cone at an angle of 120° and a load of 150kgf. Micro-hardness measurements were performed using a Shimadzu micro-hardness tester, model DUH201S, with a Vickers square diamond pyramid durometer with an angle between faces of 136° and a load of 0.25N.

2.5 Cyclic potentiodynamic assays

Samples were immersed in a 3.5% sodium chloride solution in distilled water and linear polarization tests were performed with an IVIUM brand potentiostat using a saturated calomel electrode as reference and a platinum counter electrode. The sampling rate of the linear polarization tests was 1mV/s.

2.6 Wear tests

In order to evaluate the effect of niobium on wear resistance, the "Free Ball" micro-abrasion test was performed, and the wear coefficient (K) can be calculated using Archard's equation according to **Equation 2** [23].

3. RESULTS AND DISCUSSION

The results of the optical emission spectrometry analyzes show that the steels machined belong to the family SEW 410 Nr.14517 and the contents of chromium, molybdenum and nitrogen are sufficient to promote adequate corrosion resistance.

Table 1 shows the calculation of the PREN number and the percentage of chemical elements in the super-duplex stainless steels studied according to the PREN concepts. In all 3 solubilized samples the presence of the sigma phase was not observed. After aging, it was not possible to identify carbides and nitrides in the microstructures, probably due to the low carbon and nitrogen content present in the SEW 410 steels. All 9 aged samples exhibited a sigma phase at the interfaces between ferrite and austenite due to the eutectoid decomposition of ferrite during heating at 850 °C.

Table 1: Number of PREN and chemical composition of the analyzed steels

	C	Cr	Ni	Mo	Cu	Mn	Si	N	P	S	Nb	PREN
SEW	0.03	24.0	5.0	2.5	2.8	2.0	1.0	0.12	0.03	0.02	-	39,8
standard	max.	26.5	7.0	3.5	3.5	max.	max.	0.25	max.	max.	-	49,0
0.2%Nb	0,03	25,8	6,5	3,2	2,9	1,3	0,7	0,21	0,03	0,01	0,20	45,3
0.5%Nb	0,03	25,8	6,3	3,2	3,0	1,4	0,8	0,22	0,03	0,01	0,51	45,3
1.5%Nb	0,03	25,4	6,2	3,2	2,9	1,3	0,8	0,22	0,03	0,01	1,52	44,8

The chemical composition of the sigma phase, determined by scanning electron microscopy analysis EDS, revealed a content of 54% Fe, 32% Cr, 7% Mo, 5% Ni and 2% Cu. The presence of a Laves phase was not detected in steels containing 0.2% Nb, but this phase was observed in steels containing 0.5% Nb and 1.5% Nb. The addition of niobium containing more than 0.5% Nb causes the formation of the Laves phase because favors the formation of niobium carbides (NbC and Nb₄C₃). The Laves phase has a needle-like shape randomly distributed in the microstructure, as shown in **Figure 1**.

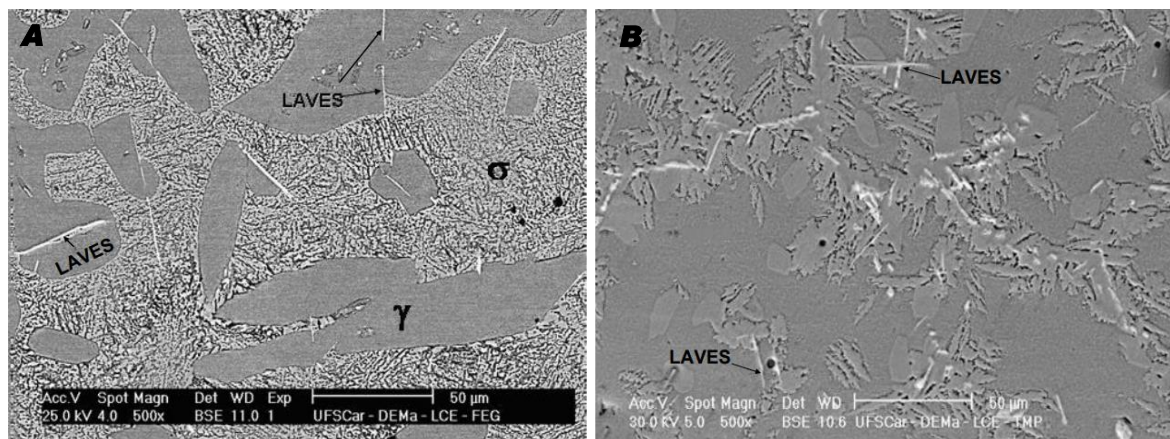


Figure 1: Laves phase in the form of needles. (A) 0.5%Nb aging at 850°C/60 min (B) 1.5%Nb solubilized at 1050°C/60 min.

Figures 2 to 4 show the volume fractions of the austenite, ferrite and sigma phases as determined by image analysis and the ferritescope. The ferritic (magnetic) phase was measured using a ferritescope, while the non-magnetic sigma phase was calculated from the percent difference between the austenitic and ferritic phases using **Equation 3**:

$$\% \text{ Sigma Phase} = 100 - (\% \text{ austenite phase} + \% \text{ ferrite phase}) \quad (3)$$

Comparing steels solubilized with 0.2% and 0.5% niobium, it is found that the addition of this element did not change the duplex matrix, since the amount of austenite in the steel with 0.5%Nb is only 4% less than in the steel with 0.5% niobium.

However, when comparing steels solubilized with 0.2% and 1.5% niobium, it can be seen that the addition of this element significantly changed the duplex matrix, as the overall austenitic matrix of the 1.5% steel decreased by about 60%.

The volumetric phase fraction measurements confirmed that after the thermal treatment of aging at 850 °C, the amount of ferrite in the modified steel with 0.2% niobium is larger compared to the steel without niobium, showing the alpha effect of the element in solution.

However, in the steel with 0.5% niobium, the amount of ferrite is less than in the modified steel with 0.2% of the element, which is due to the precipitation of the Laves phase during solidification, favored by the niobium content above the solubility limit in the matrix.

This phase, in the form of platelets as shown in Figure 1, is mainly composed of iron, niobium and chromium and does not dissolve at the usual heat treatment temperatures. Because of the precipitation of the Laves phase, the ferritic phase is destabilized by a reduction in chromium content, which favors the transformation of the sigma phase during aging at 850 °C [24, 25].

The Laves phase is almost unquantifiable and represents less than 0.1% of the total microstructure. The steel with 0.2% niobium did not exhibit Laves phase precipitation. Analyzing Figure 1A, can see that the Laves phase is very similar to a needle, while in Figure 1B these needles are thicker due to the higher niobium content.

In this family steel, the Laves phase is a precipitate due to the excess of niobium in the matrix, and this precipitate does not change with heat treatment.

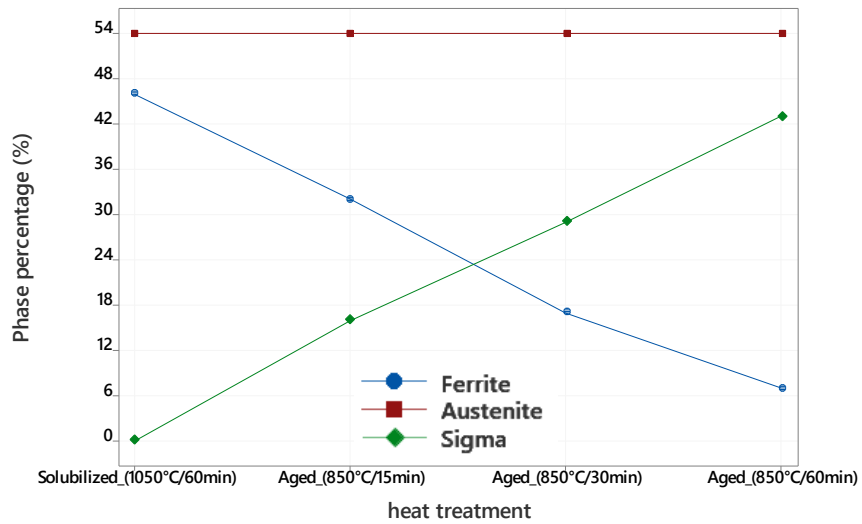


Figure 2: Volumetric percentage of the phases present in steel with 0.2%Nb

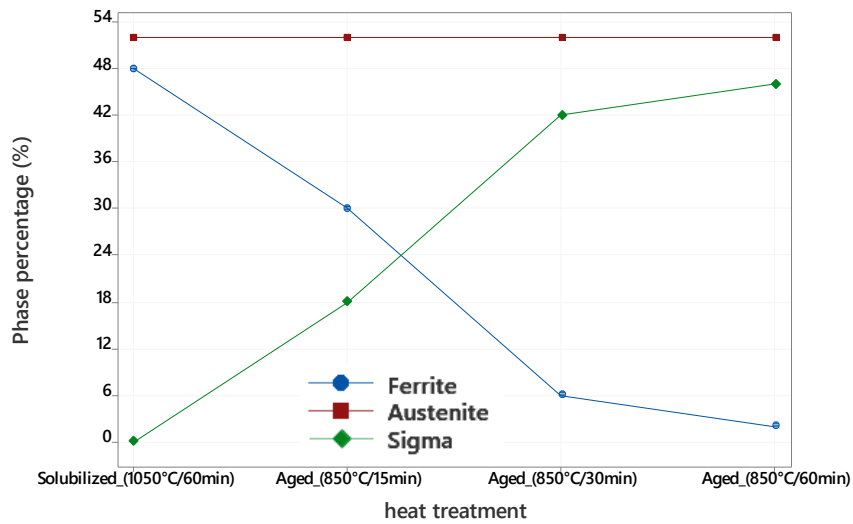


Figure 3: Volumetric percentage of the phases present in steel with 0.5%Nb

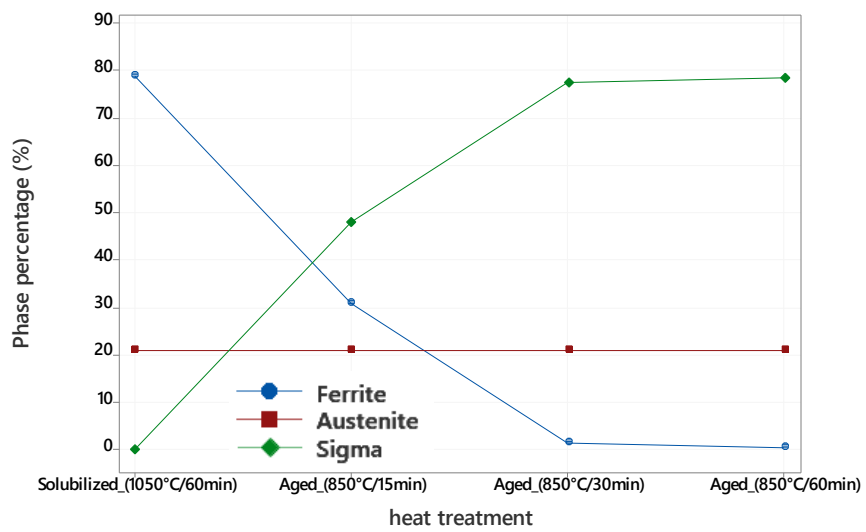


Figure 4: Volumetric percentage of the phases present in steel with 1.5%Nb

In steels with 0.5% Nb and 1.5% Nb (Figures 3 and 4), the ferrite is almost completely transformed into the sigma phase after 30 minutes of aging. In the steel modified with dissolved 1.5% Nb (Figure 4), the austenite content is lower compared to the other steels, which shows the ferritizing effect of niobium in this steel. After 30 minutes of aging, the reaction kinetics increases the instability of ferrite and it enters the sigma phase.

Several authors confirm that the sigma phase depletes the ferritic matrix in terms of chromium (Cr) and molybdenum (Mo) and that, during aging, ferrite transforms into a sigma phase from the ferrite/austenite interface. The Laves phase and the sigma phase destabilize the ferritic phase. Analyzing Figure 4, it can see only 0.5% of ferritic phase in steel with 1.5% niobium [3, 5, 11, 15-19, 26, 27].

During the cyclic potentiodynamic polarization tests, the corrosion potential of the samples with 0.5%Nb and 1.5% Nb decreased significantly compared to steels with 0.2% Nb in the dissolved and aged states. This decrease in corrosion resistance is caused by the Sigma and Laves phases [8, 19].

Figure 5 shows the behavior of the corrosion potential in volts of the investigated samples. Corrosion potential analysis shows that the corrosion resistance of steel with 0.2% Nb (Figure 5) does not decrease significantly after thermal aging treatment of 15, 30 and 60 minutes compared to other steels.

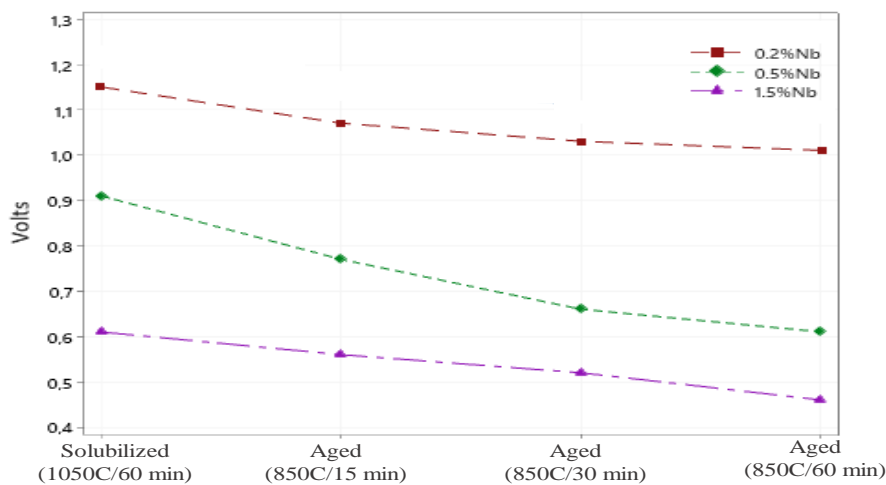


Figure 5: Effect of niobium on the corrosion potential in Volts of solubilized and aged samples

As shown in Table 1, the samples have a high number of PREN. However, PREN cannot be considered in isolation as a crucial factor in measuring the pitting resistance of stainless steel, since during aging the intermetallic phases formed reduce the corrosion resistance, as shown in Figure 5 by the precipitation of sigma and Laves phases contribute to this reduction [28-30].

Table 2 shows the values of micro-hardness and hardness measured for steels solubilized at 1050°C/60min and aged at 850°C for 15, 30 and 60 minutes.

When measuring micro-hardness, the austenite phase is easily seen under an optical microscope, unlike the sigma phase, which is associated with ferrite. In this case, the values represent regions where the sigma-associated ferrite phase is present.

The hardness of the dissolved steels is due to the hardening of the niobium in solid solution, while in the aged steels the precipitation of the sigma phase and the Laves phase are the main contributors to the increase in hardness.

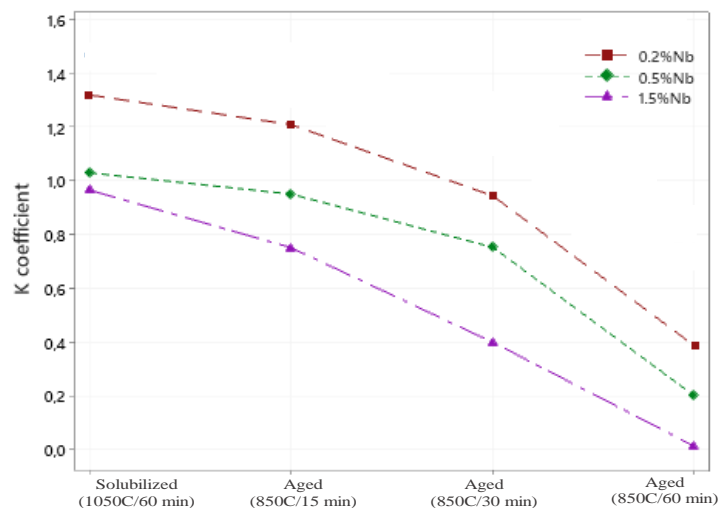
The formation of the sigma phase increased the hardness of the aged steels. Analyzing Table 2, it can be seen that the sigma phase is harder than the ferritic and authentic phases.

Figure 6 shows the values of wear coefficients for steels solubilized at 1050°C/60min and aged at 850°C for 15, 30 and 60 minutes.

The wear coefficient, in $10^{-12} \times \text{m}^2/\text{N}$, shown in Figure 6 decreases with increasing niobium content and aging time. The formation of sigma phase in conjunction with Laves phase are the main responsible for the increase in wear resistance of the steels.

Table 2: Measurement of Vickers micro-hardness (HV) and Rockwell hardness (HRC)

Sample with niobium 0.2%Nb			
Heat treatment	Ferrite + Sigma (Vickers)	Austenita (Vickers)	Rockwell Hardness C
Solubilized (1050°C/60 min)	305 ± 10	260 ± 03	24 ± 1
Aged (850°C/15 min)	340 ± 20	262 ± 05	26 ± 1
Aged (850°C/30 min)	576 ± 15	283 ± 04	28 ± 1
Aged (850°C/60 min)	692 ± 12	292 ± 03	43 ± 1
Sample with niobium 0.5%Nb			
Heat treatment	Ferrite + Sigma (Vickers)	Austenita (Vickers)	Rockwell Hardness C
Solubilized (1050°C/60 min)	314 ± 15	263 ± 05	26 ± 1
Aged (850°C/15 min)	450 ± 20	276 ± 06	28 ± 1
Aged (850°C/30 min)	576 ± 15	290 ± 04	32 ± 1
Aged (850°C/60 min)	609 ± 12	292 ± 04	47 ± 1
Sample with niobium 1.5%Nb			
Heat treatment	Ferrite + Sigma (Vickers)	Austenita (Vickers)	Rockwell Hardness C
Solubilized (1050°C/60 min)	331 ± 7	286 ± 7	27 ± 1
Aged (850°C/15 min)	579 ± 9	411 ± 14	37 ± 1
Aged (850°C/30 min)	709 ± 17	416 ± 7	41 ± 1
Aged (850°C/60 min)	731 ± 9	451 ± 16	48 ± 1


Figure 6: Values of wear coefficients (K) of solubilized and aged steels

The results also show that the wear resistance increases with decreasing corrosion resistance, i.e. the higher the content of sigma phases, the greater the wear resistance of the material.

Although the corrosion resistance decreases, the increase in hardness with the niobium content and the sigma and laves phases may favor the use of these steels in less aggressive media where wear is a factor to be minimized.

4. CONCLUSIONS

The results obtained in this investigation show that:

- Preferably at the interfaces of the sigma phase depletes the ferritic matrix in terms of chromium (Cr) and molybdenum (Mo) content;
- During aging, the ferrite at the interface transforms into a sigma phase.
- For steel containing 1.5% Nb, the matrix is essentially ferrite;
- Niobium in solution in the matrix increases the hardness of the steels;

- The increase in the niobium content, above 0.2%, favors the formation of the Laves phase;
- Increasing the niobium content decreases the corrosion resistance;
- Increasing the aging time promotes an increase in the sigma phase;
- Sigma phase and Laves phase decrease the corrosion potential;
- The Laves phase destabilizes the ferrite phase;
- The formation of the sigma phase increases the hardness of the aged steels;
- The wear coefficient (K) decreases with the increase of the niobium content and the sigma and Laves phases;

5. REFERENCES

- [1] ARAUJO, L.C.A., *et al.*, “Microbiological corrosion behavior of the duplex steel with the ammonium quaternary salts application”, *Materia Journal*, v. 24, n.1, pp. 01-12, 2019.
- [2] BORGES, F.M.R. *et al.*, “Plasma nitriding of welded joint of the SAF 2507 super duplex stainless steel”, *Materia Journal*, v. 24, n.1, pp. 01-11, 2019.
- [3] CAVALCANTI, D. A., *et al.*, “Effect of Sigma Phase Precipitated at 850 °C on Corrosion Behaviour of UNS S82441 Duplex Stainless Steel”, *Materia Journal*, v. 24, n.3, pp. 01-11, 2019.
- [4] DUAN, Z., MAN, C., DONG, C., *et al.*, “Pitting behavior of SLM 316L stainless steel exposed to chloride environments with different aggressiveness: Pitting mechanism induced by gas pores”, *Corrosion Science*, v. 162, pp. 91-112, 2020.
- [5] FONSECA, C.S., *et al.*, “Evaluation of the sigma phase precipitation susceptibility in duplex stainless steel SAF2205 welding”, *Materia Journal*, v. 24, n.3, pp. 01-09, 2019.
- [6] HAUPT, W., *et al.*, “Analysis of metallurgic transformations on UNS S31803 duplex stainless steel HAZ welded by pulsed GMAW process”, *Materia Journal*, v. 22, n.1, pp. 01-09, 2017.
- [7] ITMAN, A., FAVARATO, L.N.O., MOURA, A.N., *et al.*, “Study of the recrystallization and crystallographic texture evolution during final annealing of UNS S32304 Lean Duplex stainless steel”, *Materials Characterization*, v. 130, n. 3, pp. 39-49, 2017.
- [8] HAGHDADI, N., CIZEK, P., HODGSON, P.D., *et al.*, “Effect of ferrite-to-austenite phase transformation path on the interface crystallographic character distributions in a duplex stainless steel”, *Acta Materialia*, v. 145, pp. 196-209, 2018.
- [9] LACERDA, J.C., *et al.*, “Pitting Corrosion Behavior of UNS S31803 and UNS S32304 Duplex Stainless Steels in 3.5 wt% NaCl Solution”, *Materia Journal*, v. 25, n.2, pp. 01-10, 2020.
- [10] KUMARESH, B., ARAVIND, N., “Intergranular corrosion characteristics of niobium stabilized 27Cr-7NiMo-W-N cast hyper duplex stainless steel”, *Materials Today: Proceedings*, v. 31, n. 1, pp. 279-283, Feb. 2020.
- [11] MENDONÇA, C.S.P., *et al.*, “Influence of aging heat treatment at 850°C in the microstructure, mechanical and magnetic properties of Duplex steel UNS S3180”, *Materia Journal*, v. 18, n.3, pp. 01-09, 2013.
- [12] SCHMID, A., MORI, G., STEFAN, H., *et al.*, “Comparison of the high-temperature chloride-induced corrosion between duplex steel and Ni based alloy in presence of H₂S”, *Corrosion Science*, v. 139, pp. 76-82, Apr. 2018.
- [13] SERRA, P.L.C., *et al.*, “Study of plasma nitriding and duplex treatment on high speed steel drills”, *Materia Journal*, v. 25, n.2, pp. 01-15, 2020.
- [14] TORRES, C.E., *et al.*, “Corrosion failures of austenitic and duplex stainless steels in a biodiesel plant”, *Materia Journal*, v. 25, n.2, pp. 01-11, 2020.
- [15] HOULONG, L., LIANGLIANG, W., MINGYU, M., *et al.*, “Laves phase precipitation behavior and high-temperature strength of W-containing ferritic stainless steels”, *Journal of Materials Science & Technology*, v. 30, n. 2, pp. 179-187, Dec. 2019.
- [16] HUI-HU, L., HONG-KUI, G., WEI, L., “High-temperature Laves precipitation and its effects on recrystallisation behaviour and Lüders deformation in super ferritic stainless steels”, *Materials and Design*, v. 188, pp. 1-12, Mar. 2020.
- [17] LIANG, Y., YAN, W. SHI, X., *et al.*, “On Laves phase in a 9Cr3W3CoB martensitic heat resistant steel when aged at high temperatures”, *Journal of Materials Science & Technology*, v. 85, pp. 129-140, 2021.
- [18] SHANG, S., JING, C., ZUO, L., *et al.*, “Investigation of dissolution behavior of laves phase in inconel 718 fabricated by laser directed energy deposition”, *Additive Manufacturing*, v. 32, pp. 1-12, Jan. 2020.
- [19] TODA, Y., NAKAMURA, Y., HARADA, N., *et al.*, “Effect of the Laves phase and carbide on the creep strength of Fe–15Cr–W alloys”, *Materials Science and Engineering: A*, v. 797, pp. 140104, 2020.
- [20] MAGNABOSCO, R., CAMILA, H.B., WILMAR, C.H., *et al.*, “Effect of Aging Heat Treatment H950 and H1000 on Mechanical and Pitting Corrosion Properties of UNS S46500 Stainless Steel”, *Materials Research*, v. 22, n. 1, pp. 1-9, Jan. 2019.

- [21] YANG Y., LIU, L., BI, H. *et al.*, “Corrosion evolution of 2205 duplex stainless steel in hot concentrated seawater under intermittent vacuum and boiling conditions”, *Corrosion Science*, v.1, pp. 109881, 2021.
- [22] ZHIQIANG, Z., HONGYANG, J., LIANYONG X., *et al.*, “Effect of post-weld heat treatment on microstructure evolution and pitting corrosion resistance of electron beam-welded duplex stainless steel”, *Corrosion Science*, v. 141, pp. 30-45, Jul. 2018.
- [23] GOBBI, V.J., GOBBI, S.J., SILVA, C.R.M. “Nitriding the influence of plasma in resistance to wear microabrasive tool steel AISI D2”, *ABM proceedings*, v.1, pp. 01-12, 2021.
- [24] ZHI, Y., JIE, P., ZIXIE, W., *et al.*, “Plasticity improvement of Fe-13Cr-6Al-2Mo-0.5Nb alloy with yttrium addition by hindering Laves phase precipitation”, *Materials Characterization*, v. 170, pp. 110647, 2020.
- [25] ZUO, A., SHAO, C., HUO, X., *et al.*, “Study on the Laves phase precipitation behavior and its effect on toughness of 10Cr-1Mo steel weld joint after thermal aging”, *Journal of Manufacturing Processes*, v.64, pp. 1287-1295, 2021.
- [26] ZHU, C., WANG, W., CHANG, S., *et al.*, “Mechanism of $\delta \rightarrow \delta + \gamma$ phase transformation and hardening behavior of duplex stainless steel via sub-rapid solidification process”, *Materials Characterization*, v. 170, pp. 110679, 2020.
- [27] ZHANG, J. HU, X., CHOU, K. “In-situ environmental transmission electron microscopy investigation of the phase transformation austenite \rightarrow ferrite in duplex stainless steel”, *Materials Letters*, v. 264, pp. 127259, 2020.
- [28] DUBIELA, S.M., ŻUKROWSKI, J., “Phase decomposition at 402°C in an Fe-Cr alloy: Mössbauer spectroscopic study”, *Materials Characterization*, v. 129, pp. 282-287, May. 2017.
- [29] NOGUEIRA, P.H.B.O., *et al.*, “Influence of H₂S on the formation and reconstruction of passive layer of Super 13Cr steel in simulated deep water oil exploration media”, *Materia Journal*, v. 25, n.2, pp. 01-11, 2020.
- [30] WILMAR, C.H., “Effect of sulfate on the pitting potential of austenitic stainless steels 18Cr8Ni and 17Cr6Mn5Ni in chloride media”, *REM: R. Esc. Minas, Ouro Preto*, v. 72, n. 1, pp. 97-103, Marc. 2019.

ORCIDWanderleiton da Silva Cardoso <https://orcid.org/0000-0001-8531-4049>Raphael Colombo Baptista <https://orcid.org/0000-0003-0784-6861>